

(2-(Dimethylammonium)ethyl)cyclopentadienyltricarbonylmetalates: Group VI Metal Zwitterions. Attenuation of the Brønsted Basicity and Nucleophilicity of Formally Anionic Metal Centers

Paul J. Fischer,^{*,†} Kristina M. Krohn,[†] Edward T. Mwenda,[†] and Victor G. Young, Jr.[‡]

Department of Chemistry, Macalester College, Saint Paul, Minnesota 55105-1899, and Department of Chemistry, X-ray Crystallographic Laboratory, University of Minnesota, Minneapolis, Minnesota 55455-0431

Received June 11, 2005

Protonation of (2-(dimethylamino)ethyl)cyclopentadienyl (Cp^N) group VI metal carbonyl anions with acetic acid proceeds at the amine to provide zwitterionic (2-(dimethylammonium)ethyl)cyclopentadienyltricarbonylmetalates, M(CO)₃(η⁵-Cp^{NH}) (M = Cr (**1**), Mo (**2**), W (**3**)). Few zwitterionic organometalates with anionic metal centers and positive charges that cannot be delocalized have been reported to date. The impact of the intramolecular charge separation on the structures and reactivity of zwitterionic organometalates is of current interest. The M(CO)₃ units of structurally characterized **1–3** are significantly perturbed in solution and the solid state due to ion-pairing between the pendant ammonium cation and anionic metal center. The concentration and solvent dependence of the ¹H NMR ammonium hydrogen chemical shifts of **1–3** and the intramolecular N⋯M separations of these zwitterions in the solid state are consistent with three-center–four-electron N–H⋯M hydrogen bonding. One other hydrogen bond with a zerovalent group VI metal acceptor has been characterized to date. The intramolecular charge separation attenuates the reactivity of the anionic metal centers of **1–3** relative to that of [M(CO)₃(η⁵-Cp)]⁻. Structurally characterized [WH(CO)₃(η⁵-Cp^{NH})]Cl (**4**) was the only isolable salt obtained from protonation of **1–3**; the Cr and Mo analogues are unstable relative to **1** and **2**, respectively. Structurally characterized [M(AuPPh₃)(CO)₃(η⁵-Cp^{NH})]Cl (M = Mo (**5**), W(**6**)) were synthesized via reactions of **2** and **3**, respectively, with Ph₃PAuCl and protonation of M(AuPPh₃)(CO)₃(η⁵-Cp^N) (M = Mo (**8**), W (**9**)) with HCl. Pure samples of the analogous chromium salt were inaccessible from either **1** or structurally characterized Cr(AuPPh₃)(CO)₃(η⁵-Cp^N) (**7**).

Introduction

Zwitterionic organometalates exhibit interesting structures and reactivity due to the electronic impact of their formal charge separation.¹ Consideration of zwitterions is important in transition metal catalyst design. The catalytic activity of bis(cyclopentadienyl) complexes with cationic group IV metal centers and intramolecular anionic functions (e.g., Cp*₂Zr(*m*-C₆H₄-BPh₃)₂,^{2a} (Cp*)₂(C₅Me₄CH₂B(C₆F₅)₃)Zr(C₆H₅)₂^{2b}) depends on the interaction between the opposite charges permitted by the structure.^{2c–h} Zwitterions with anionic

metal centers have received relatively less attention to date despite speculation that specifically designed intramolecular dative-electrostatic interactions in the coordination sphere of reduced metal centers could govern catalyst activity or selectivity.^{1,3} Among these zwitterions with a single metal, many feature conjugated ligands that allow negative charge delocalization (e.g., W(CO)₅{C=C(Ph)CH(Ph)CH=CHN(*i*Pr)=C(OEt)},^{4a–c} MoO(SC₆H₂*i*Pr_{3-2,4,6})₃{=C(Ph)CH=C(Ph)-CH₂PMe₂Ph}^{4d}). The incorporation of an sp³ carbon between group VI metal pentacarbonyl units and conjugated systems (e.g., W(CO)₅{CHN(*n*Pr)=C(OMe)CH=C(Ph)NCH=CHCH=C}^{4e}) allows delocalization of posi-

* To whom correspondence should be addressed. E-mail: fischer@macalester.edu.

[†] Macalester College.

[‡] University of Minnesota.

(1) Chauvin, R. *Eur. J. Inorg. Chem.* **2000**, 577.

(2) (a) Hlatky, G. G.; Turner, H. W.; Eckman, R. R. *J. Am. Chem. Soc.* **1989**, *111*, 2728. (b) Sun, Y.; Spence, R. E. v. H.; Piers, W. E.; Parvez, M.; Yap, G. P. A. *J. Am. Chem. Soc.* **1997**, *119*, 5132. (c) Piers, W. E. *Chem. Eur. J.* **1998**, *4*, 13. (d) Bochmann, M. *Top. Catal.* **1999**, *7*, 9. (e) Piers, W. E.; Sun, Y.; Lee, L. W. M. *Top. Catal.* **1999**, *7*, 133. (f) Karl, J.; Erker, G.; Fröhlich, R.; Zippel, F.; Bickelhaupt, F.; Schreuder Goedheijt, M.; Akkerman, O. S.; Binger, P.; Stannek, J. *Angew. Chem., Int. Ed. Engl.* **1997**, *36*, 2771. (g) van der Heijden, H.; Hessen, B.; Orpen, A. G. *J. Am. Chem. Soc.* **1998**, *120*, 1112. (h) Cowley, A. H.; Hair, G. S.; McBurnett, B. G.; Jones, R. A. *Chem. Commun.* **1999**, 437.

(3) (a) Brunet, J.-J.; Chauvin, R.; Commenges, G.; Donnadiou, B.; Leglaye, P. *Organometallics* **1996**, *15*, 1752. (b) Brunet, J.-J.; Chauvin, R.; Chiffre, J.; Huguet, S.; Leglaye, P. *J. Organomet. Chem.* **1998**, *566*, 117.

(4) (a) Aumann, R.; Nienaber, H. *Adv. Organomet. Chem.* **1997**, *41*, 163. (b) Aumann, R.; Yu, Z.; Fröhlich, R.; Zippel, F. *Eur. J. Inorg. Chem.* **1998**, 1623. (c) Aumann, R.; Yu, Z.; Fröhlich, R. *J. Organomet. Chem.* **1997**, *549*, 311. (d) Fairhurst, S. A.; Hughes, D. L.; Marjani, K.; Richards, R. L. *J. Chem. Soc., Dalton Trans.* **1998**, 1899. (e) Barluenga, J.; Tomás, M.; Rubio, E.; López-Pelegrín, J. A.; García-Granda, S.; Pérez Priede, M. *J. Am. Chem. Soc.* **1999**, *121*, 3065. (f) Aumann, R.; Fröhlich, R.; Prigge, J.; Meyer, O. *Organometallics* **1999**, *18*, 1369.

tive charge but permits retention of anionic metal fragments in all resonance structures.^{4f} Zwitterionic organometalates that feature a single anionic metal and a positive charge that cannot be delocalized are rare, and these complexes exhibit fascinating properties. Despite the formal negative charge on tungsten in the zwitterionic olefin-coordinated imine complex $W(CO)_2-(\eta^2-(Z)-(Me_2N=C(Me))CH=CHCOOH)(\eta^5-Cp)$, the metal neither deprotonates the carboxylic acid nor can be methylated by CH_3I .⁵ Zwitterionic $HfFe(CO)_3(PPh_2OCH(Ph)CH(Me)NMe_3)$ exhibits an unexpected cis H–Fe–P geometry to permit close contact between NMe_3^+ and $[HfFe]^-$ in the vicinity of the hydride.^{3a}

Zwitterionic organometalates have played an important role in establishing the existence of hydrogen bonds where transition metals function as acceptors.⁶ The negatively charged platinum and dimethylammonium substituent of $PtBr(C,N-8-C_{10}H_6NMe_2)(C-8-C_{10}H_6NMe_2H)$ participate in a N–H···Pt hydrogen bond.⁷ Many three-center–four-electron X–H···M hydrogen bonds have been characterized with electron-rich d^8 and d^{10} metal centers.⁶ Only one hydrogen bond involving a zerovalent group VI metal acceptor has been reported to date. An intramolecular O–H···Mo hydrogen bond in the η^6 -arene complex $Mo(PEt_3)_3(\eta^6-C_6H_5C_6H_3(Ph)OH)$ was confirmed by Parkin in both solution and the solid state.⁸

Our research group is exploring the chemistry of (2-(dimethylamino)ethyl)cyclopentadienyl (Cp^N) metal carbonyl anions. The reactivity of transition metal Cp^N complexes in which both the pendant amine and metal center are susceptible to electrophilic attack is an area of current interest.⁹ The lack of constraints on the amine is not conducive to an intramolecular N–Sn interaction in the tin(IV) derivatives $M'(SnR_3)(CO)_3(\eta^5-Cp^N)$ ($M' = Mo, W; R = Ph, cyclohexyl$).¹⁰ The basicities of $[M(CO)_3(\eta^5-Cp)]^-$ ($M = Cr, Mo, W$) determined by Norton and Jordan¹¹ suggested that protonation of the group VI metal anions $[M(CO)_3(\eta^5-Cp^N)]^-$ would occur at the tertiary amine and provide zwitterionic organometalates $M(CO)_3(\eta^5-Cp^{NH})$. We have synthesized and characterized these zwitterions in solution and the solid state. The surprisingly unreactive tungsten center of $W(CO)_2-(\eta^2-(Z)-(Me_2N=C(Me))CH=CHCOOH)(\eta^5-Cp)$ prompted us to explore the metal-based reactivity of these zwitterions toward protonation and electrophilic addition with triphenylphosphinegold(I) chloride.

Experimental Section

General Procedures. All operations were performed under an atmosphere of 99.5% argon further purified by passage

(5) (a) Butters, C.; Carr, N.; Deeth, R. J.; Green, M.; Green, S. M.; Mahon, M. F. *J. Chem. Soc., Dalton Trans.* **1996**, 2299. (b) Lee, L.; Chen, D.-J.; Lin, Y.-C.; Lo, Y.-H.; Lin, C. H.; Lee, G.-H.; Wang, Y. *Organometallics* **1997**, *16*, 4636.

(6) (a) Brammer, L. *J. Chem. Soc., Dalton Trans.* **2003**, 3145, and references therein. (b) Martín, A. *J. Chem. Educ.* **1999**, *76*, 578, and references therein.

(7) Wehman-Ooyevaar, I. C. M.; Grove, D. M.; Kooijman, H.; van der Sluis, P.; Spek, A. L.; van Koten, G. *J. Am. Chem. Soc.* **1992**, *114*, 9916.

(8) Hascall, T.; Baik, M.-H.; Bridgewater, B. M.; Shin, J. H.; Churchill, D. G.; Friesner, R. A.; Parkin, G. *Chem. Commun.* **2002**, 2644.

(9) Esteruelas, M. A.; López, A. M.; Oñate, E.; Royo, E. *Inorg. Chem.* **2005**, *44*, 4094.

(10) Fischer, P. J.; Krohn, K. M.; Mwenda, E. T.; Young, V. G., Jr. *Organometallics* **2005**, *24*, 1776.

(11) Jordan, R. F.; Norton, J. R. *J. Am. Chem. Soc.* **1982**, *104*, 1255.

through a column of activated Aceto Corp. catalyst R3-11 and 10 Å molecular sieves. The plumbing components of the gas purification systems were made of glass and copper. Ultra-Torr and Swagelok fittings were employed to provide connections between glass and copper tubing that are impermeable to air. Solutions were routinely transferred via stainless steel cannulas. Gastight syringes equipped with stainless steel three-way stopcocks and needles were used to transfer solutions when necessary. Standard Schlenk techniques were employed with double manifold vacuum lines.¹² Solids were handled in a glovebox. Solvents were purified by standard procedures and stored under argon. Literature procedures were employed to prepare $NaCp^N$ and triphenylphosphinegold(I) chloride.^{13,14} The reagents $M(CO)_6$ ($M = Cr, Mo, W$), concentrated aqueous HCl, trifluoroacetic acid, phosphoric acid, and glacial acetic acid were used as received (Aldrich). Solution infrared spectra were acquired on a Nicolet Magna 550 FTIR spectrometer with samples sealed in 0.1 mm gastight NaCl cells. Nujol (mineral oil) mulls for IR spectra were prepared in the glovebox. NMR samples were sealed under argon into 5 mm tubes and were analyzed on a Varian Gemini 300 MHz FT-NMR spectrometer at ambient temperature. 1H and ^{13}C chemical shifts are reported in parts per million (δ) and are given with reference to residual 1H and ^{13}C solvent references relative to TMS. Melting points (uncorrected) were determined under argon in sealed capillary tubes on a Laboratory Devices Mel-Temp apparatus. Microanalyses were carried out by H. Malissa and G. Reuter Analytische Laboratorien, Lindlar, Germany.

Similar procedures were conducted to synthesize **1–3**, **5–6**, and **7–9**, respectively. Representative procedures for **1**, **5**, and **7** are provided below. Complete experimental details for **2**, **3**, **6**, **8**, and **9** are given in the Supporting Information.

Cr(CO)₃(η^5 -Cp^{NH}) (1). CH_3CN (70 mL) was added to $Cr(CO)_6$ (0.754 g, 3.43 mmol) and $NaCp^N$ (0.600 g, 3.77 mmol). The pale yellow solution was refluxed for 52 h. The CH_3CN was removed in vacuo, and THF (70 mL) was added to provide a red-orange solution. Addition of a 20% v/v glacial acetic acid/THF solution (1.20 mL containing 0.252 g, 4.19 mmol of $HC_2H_3O_2$) at ambient temperature resulted in a dark orange suspension; the $[Cr(CO)_3(\eta^5-Cp^N)]^-$ was consumed within 15 min. The suspension was filtered through Celite. The filtrate was concentrated in vacuo until ~3 mL remained. An orange solid precipitated upon addition of Et_2O (70 mL). The nearly colorless supernatant was removed. The solid was washed with Et_2O (2×50 mL) and dried in vacuo. Recrystallization from CH_3CN/Et_2O provided orange, air-sensitive microcrystals (0.634 g, 68%). Anal. Calcd for $C_{12}H_{15}CrNO_3$: C, 52.75; H, 5.53; N, 5.13. Found: C, 52.55; H, 5.52; N, 5.31. Mp: 204–205 °C (dec). IR (CH_3CN) $\nu(CO)$: 1906 (s), 1805 (m), 1782 (s) cm^{-1} ; (THF) $\nu(CO)$: 1910 (s), 1814 (s), 1784 (s) cm^{-1} ; (CH_2Cl_2) $\nu(CO)$: 1908 (s), 1811 (s), 1778 (s) cm^{-1} ; (Nujol) $\nu(CO)$: 1896 (s), 1801 (s), 1789 (s, sh) cm^{-1} . 1H NMR (CD_3CN , 300 MHz): δ 10.34 (s, br, 1H, NH), 4.65 (app t, $J = 2.1$ Hz, 2H, Cp), 4.41 (app t, $J = 2.1$ Hz, 2H, Cp), 3.07 (t, $J = 6.0$ Hz, 2H, CH_2CH_2N), 2.91 (s, 6H, CH_3), 2.65 (t, $J = 6.0$ Hz, 2H, CH_2CH_2N). $^{13}C\{^1H\}$ NMR (CD_3CN , 75 MHz): δ 244.1 (s, CO), 92.1 (s, quaternary C, Cp), 86.2 (s, Cp), 81.8 (s, Cp), 57.6 (s, CH_2CH_2N), 43.9 (s, CH_3), 23.3 (s, CH_2CH_2N). 1H NMR (C_4D_8O , 300 MHz): δ 11.79 (s, br, 1H, NH). $^{13}C\{^1H\}$ NMR (C_4D_8O , 75 MHz): δ 243.3 (s, CO). 1H NMR (CD_2Cl_2 , 300 MHz): δ 12.15 (s, br, 1H, NH). $^{13}C\{^1H\}$ NMR (CD_2Cl_2 , 75 MHz): δ 243.1 (s, CO).

(12) (a) Shriver, D. F.; Drezdon, M. A. *The Manipulation of Air-Sensitive Compounds*, 2nd ed.; Wiley-Interscience: New York, 1986. (b) Ellis, J. E. *ACS Symp. Ser.* **1987**, *No. 357*, 34.

(13) $NaCp^N$: (a) Bradley, S.; Corradi, M. M.; Camm, K. D.; Furtado, S. J.; McGowan, P. C.; Mumtaz, R.; Thornton-Pett, M. *J. Organomet. Chem.* **2002**, *656*, 49. (b) Rees, W. S., Jr.; Dippel, K. A. *Org. Prep. Proc. Int.* **1992**, *24*, 527.

(14) Ph_3PAuCl : Braunstein, P.; Lehner, H.; Matt, D. *Inorg. Synth.* **1990**, *27*, 218.

Mo(CO)₃(η^5 -Cp^{NH})(2). Yield: 76%. Anal. Calcd for C₁₂H₁₅-MoNO₃: C, 45.44; H, 4.77; N, 4.42. Found: C, 45.25; H, 4.78; N, 4.50. Mp: 221–222 °C (dec). IR (CH₃CN) ν (CO): 1911 (s), 1809 (s), 1788 (s) cm⁻¹; (THF) ν (CO): 1915 (s), 1819 (s), 1790 (s) cm⁻¹; (CH₂Cl₂) ν (CO): 1913 (s), 1815 (s), 1784 (s) cm⁻¹; (Nujol) ν (CO): 1900 (s), 1798 (s), 1771 (s) cm⁻¹. ¹H NMR (CD₃-CN, 300 MHz): δ 9.20 (s, br, 1H, NH), 5.25 (app t, *J* = 2.1 Hz, 2H, Cp), 5.03 (app t, *J* = 2.1 Hz, 2H, Cp), 3.02 (t, *J* = 6.3 Hz, 2H, CH₂CH₂N), 2.85 (s, 6H, CH₃), 2.74 (t, *J* = 6.3 Hz, 2H, CH₂-CH₂N). ¹³C{¹H} NMR (CD₃CN, 75 MHz): δ 234.0 (s, CO), 96.8 (s, quaternary C, Cp), 90.4 (s, Cp), 85.9 (s, Cp), 57.7 (s, CH₂CH₂N), 43.7 (s, CH₃), 23.5 (s, CH₂CH₂N). ¹H NMR (C₄D₈O, 300 MHz): ¹H δ 11.48 (s, br, 1H, NH). ¹³C{¹H} NMR (C₄D₈O, 75 MHz): δ 232.9 (s, CO). ¹H NMR (CD₂Cl₂, 300 MHz): δ 11.90 (s, br, 1H, NH). ¹³C{¹H} NMR (CD₂Cl₂, 75 MHz): δ 232.6 (s, CO).

W(CO)₃(η^5 -Cp^{NH})(3). Yield: 60%. Anal. Calcd for C₁₂H₁₅-NO₃W: C, 35.58; H, 3.73; N, 3.46. Found: C, 35.41; H, 3.68; N, 3.47. Mp: 203–204 °C (dec). IR (CH₃CN) ν (CO): 1904 (s), 1803 (s), 1782 (s) cm⁻¹; (THF) ν (CO): 2015 (m), 1920 (s), 1909 (s), 1813 (s), 1785 (s) cm⁻¹; (CH₂Cl₂) ν (CO): 2017 (m), 1920 (s, sh), 1907 (s), 1809 (s), 1779 (s) cm⁻¹; (Nujol) ν (CO): 1905 (s, sh), 1894 (s), 1791 (s), 1763 (s) cm⁻¹. ¹H NMR (CD₃CN, 300 MHz): δ 8.80 (s, br, 1H, NH), 5.27 (app t, *J* = 2.4 Hz, 2H, Cp), 5.06 (app t, *J* = 2.4 Hz, 2H, Cp), 3.01 (t, *J* = 6.3 Hz, 2H, CH₂CH₂N), 2.83 (s, 6H, CH₃), 2.81 (t, *J* = 6.3 Hz, 2H, CH₂-CH₂N). ¹³C{¹H} NMR (CD₃CN, 75 MHz): δ 224.6 (s, CO), (¹⁸³W–¹³C satellites: 226.54, 224.00, ¹J_{WC} = 192 Hz), 96.8 (s, quaternary C, Cp), 89.1 (s, Cp), 84.9 (s, Cp), 58.4 (s, CH₂CH₂N), 44.4 (s, CH₃), 24.1 (s, CH₂CH₂N). ¹³C{¹H} NMR (C₄D₈O, 75 MHz): δ 221.4 (s, CO). ¹³C{¹H} NMR (CD₂Cl₂, 75 MHz): δ 221.0 (s, CO).

[WH(CO)₃(η^5 -Cp^{NH})]Cl (4). A 5% v/v concentrated aqueous HCl/CH₃CN solution (2.40 mL containing 0.053 g, 1.46 mmol of HCl) was added to a pale yellow solution of W(CO)₃(η^5 -Cp^{NH}) (0.500 g, 1.23 mmol) in CH₃CN (50 mL). The solution immediately became colorless; the W(CO)₃(η^5 -Cp^{NH}) was consumed within 5 min. The solution was filtered through Celite, and the filtrate was concentrated in vacuo until ~4 mL remained. Dilution with Et₂O (80 mL) resulted in the precipitation of a white solid. The supernatant was removed. The solid was washed with Et₂O (3 \times 30 mL) and dried in vacuo. Recrystallization from CH₃CN/Et₂O provided white, moderately air-sensitive microcrystals (0.380 g, 70%). Anal. Calcd for C₁₂H₁₆NO₃ClW: C, 32.64; H, 3.65; N, 3.17. Found: C, 32.78; H, 3.70; N, 3.20. Mp: 168–169 °C (dec). IR (CH₃CN) ν (CO): 2019 (s), 1923 (s) cm⁻¹; (CH₃OH) ν (CO): 2021 (s), 1929 (s) cm⁻¹; (Nujol) ν (CO): 2026 (s), 1947 (s), 1889 (s) cm⁻¹. ¹H NMR (CD₃-CN, 300 MHz): δ 12.29 (s, br, 1H, NH), 5.65 (s, br, 2H, Cp), 5.46 (s, br, 2H, Cp), 3.12–2.90 (m, 4H, CH₂CH₂), 2.72 (s, 6H, CH₃), -7.25 (s, br, 1H, WH). ¹H NMR (CD₃OD, 300 MHz): δ NH not observed due to exchange with solvent, 5.80 (app t, *J* = 2.1 Hz, 2H, Cp), 5.57 (app t, *J* = 2.10 Hz, 2H, Cp), 3.35–3.25 (s, 4H, CH₂CH₂), 2.93 (s, 6H, CH₃), -7.23 (s, integrates to <1H due to exchange with solvent, WH (¹⁸³W–¹H satellites: -7.17, -7.30, ¹J_{WH} = 39 Hz)). ¹³C{¹H} NMR (CD₃OD, 75 MHz): δ 218.4 (s, br, CO), 109.0 (s, quaternary C, Cp), 91.2 (s, Cp), 89.2 (s, Cp), 60.3 (s, CH₂CH₂N), 43.8 (s, CH₃), 25.2 (s, CH₂CH₂N).

[Mo(AuPPh₃)(CO)₃(η^5 -Cp^{NH})]Cl (5). A solution of triphenylphosphinegold(I) chloride (0.319 g, 0.645 mmol) in CH₃-CN (125 mL) was added to a yellow solution of Mo(CO)₃(η^5 -Cp^{NH}) (0.205 g, 0.646 mmol) in CH₃CN (10 mL). The Mo(CO)₃(η^5 -Cp^{NH}) was consumed within 10 min. The solution was filtered through Celite. CH₃CN was removed in vacuo from the filtrate until ~5 mL remained and a pale yellow, microcrystalline solid had precipitated. Dilution with Et₂O (60 mL) resulted in additional precipitation. The supernatant was removed. The solid was washed with Et₂O (3 \times 50 mL) and dried in vacuo. Recrystallization from CH₃CN/Et₂O provided pale yellow, air-sensitive microcrystals (0.315 g, 60%). Anal. Calcd for C₃₀H₃₀-

AuClMoNO₃P: C, 44.38; H, 3.72; N, 1.73. Found: C, 44.30; H, 3.71; N, 1.88. Mp: 192–193 °C (dec). IR (CH₃CN) ν (CO): 1947 (s), 1910 (vw), 1857 (m, sh), 1837 (s) cm⁻¹; (THF) ν (CO): 1948 (s), 1917 (w), 1864 (m, sh), 1843 (s) cm⁻¹; (Nujol) ν (CO): 1948 (s), 1864 (m), 1813 (s) cm⁻¹. ¹H NMR (CD₃CN, 300 MHz): δ 7.62–7.52 (m, 15H, AuPPh₃), 5.48 (app t, *J* = 2.1 Hz, 2H, Cp), 5.27 (app t, *J* = 2.1 Hz, 2H, Cp), 2.82–2.65 (m, 4H, CH₂CH₂), 2.37 (s, 6H, CH₃). ¹³C{¹H} NMR (CD₃CN, 75 MHz): δ 232.2 (s, CO), 134.8 (d, ²J_{PC} = 14.2 Hz, *ortho* C, AuPPh₃), 132.5 (d, ⁴J_{PC} = 2.4 Hz, *para* C, AuPPh₃), 131.2 (d, ¹J_{PC} = 51.2 Hz, *ipso* C, AuPPh₃), 130.3 (d, ³J_{PC} = 10.7 Hz, *meta* C, AuPPh₃), 93.4 (s, quaternary C, Cp), 88.9 (s, Cp), 87.8 (s, Cp), 60.2 (s, CH₂CH₂N), 44.0 (s, CH₃), 26.2 (s, CH₂CH₂N).

[W(AuPPh₃)(CO)₃(η^5 -Cp^{NH})]Cl (6). Yield: 61%. Anal. Calcd for C₃₀H₃₀AuClNO₃PW: C, 40.04; H, 3.36; N, 1.56. Found: C, 40.09; H, 3.39; N, 1.61. Mp: 209–210 °C (dec). IR (CH₃CN) ν (CO): 1943 (s), 1850 (m, sh), 1831 (s) cm⁻¹; (Nujol) ν (CO): 1944 (s), 1861 (m), 1808 (s) cm⁻¹. ¹H NMR (CD₃CN, 300 MHz): δ 7.62–7.50 (m, 15H, AuPPh₃), 5.57 (app t, *J* = 2.1 Hz, 2H, Cp), 5.35 (app t, *J* = 2.1 Hz, 2H, Cp), 2.66 (s, br, 4H, CH₂CH₂N), 2.25 (s, 6H, CH₃). ¹³C{¹H} NMR (CD₃CN, 75 MHz): δ 221.8 (s, CO), 134.8 (d, ²J_{PC} = 14.6 Hz, *ortho* C, AuPPh₃), 132.5 (d, ⁴J_{PC} = 2.4 Hz, *para* C, AuPPh₃), 131.5 (d, ¹J_{PC} = 50.2 Hz, *ipso* C, AuPPh₃), 130.3 (d, ³J_{PC} = 11.2 Hz, *meta* C, AuPPh₃), 93.4 (s, quaternary C, Cp), 87.8 (s, Cp), 86.4 (s, Cp), 60.9 (s, CH₂CH₂N), 44.5 (s, CH₃), 26.8 (s, CH₂CH₂N).

Cr(AuPPh₃)(CO)₃(η^5 -Cp^N)(7). CH₃CN (100 mL) was added to Cr(CO)₆ (0.377 g, 1.71 mmol) and NaCp^N (0.300 g, 1.88 mmol). The pale yellow solution was refluxed for 50 h. The CH₃CN was removed in vacuo; the residue was dissolved in THF (60 mL) to provide an orange solution. A solution of triphenylphosphinegold(I) chloride (0.847 g, 1.71 mmol) was added, resulting in a bright yellow solution; the [Cr(CO)₃(η^5 -Cp^N)]⁻ was consumed within 10 min. The solution was filtered through alumina. The filtrate was concentrated in vacuo. The resulting red oil was dissolved in Et₂O (70 mL) and filtered. The filtrate was concentrated in vacuo until ~3 mL remained. The addition of pentane (100 mL) precipitated a red-orange oil. Trituration converted this oil into a yellow solid, which was isolated by filtration, washed with pentane (3 \times 10 mL), and dried in vacuo. Recrystallization from Et₂O/pentane resulted in a brownish yellow, air-stable powder (0.700 g, 56%). Anal. Calcd for C₃₀H₂₉AuCrNO₃P: C, 49.26; H, 4.00; N, 1.91. Found: C, 49.34; H, 3.96; N, 2.04. Mp: 97–98 °C (dec). IR (THF) ν (CO): 1935 (s), 1856 (m, sh), 1828 (s) cm⁻¹; (Et₂O) ν (CO): 1940 (s), 1861 (m), 1833 (s) cm⁻¹; (Nujol) ν (CO): 2002 (w), 1924 (s), 1869 (w), 1832 (s, sh), 1814 (s) cm⁻¹. ¹H NMR (CD₂Cl₂, 300 MHz): δ 7.62–7.44 (m, 15H, AuPPh₃), 4.85 (app t, *J* = 2.1 Hz, 2H, Cp), 4.71 (app t, *J* = 2.1 Hz, 2H, Cp), 2.41 (m, 4H, CH₂CH₂N), 2.12 (s, 6H, CH₃). ¹³C{¹H} NMR (CD₂Cl₂, 75 MHz): δ 240.2 (s, CO), 134.6 (d, ²J_{PC} = 14.2 Hz, *ortho* C, AuPPh₃), 131.9 (s, br, *para* C, AuPPh₃), 130.7 (d, ¹J_{PC} = 50.8 Hz, *ipso* C, AuPPh₃), 129.7 (d, ³J_{PC} = 11.2 Hz, *meta* C, AuPPh₃), 106.1 (s, quaternary C, Cp), 84.1 (s, Cp), 83.1 (s, Cp), 61.2 (s, CH₂CH₂N), 45.7 (s, CH₃), 27.9 (s, CH₂CH₂N).

Mo(AuPPh₃)(CO)₃(η^5 -Cp^N)(8). Yield: 45%. Anal. Calcd for C₃₀H₂₉AuMoNO₃P: C, 46.47; H, 3.77; N, 1.81. Found: C, 46.57; H, 3.75; N, 1.85. Mp: 87–88 °C (dec). IR (THF) ν (CO): 1947 (s), 1862 (m, sh), 1840 (s) cm⁻¹; (Nujol) ν (CO): 1944 (s), 1843 (s, sh), 1824 (s) cm⁻¹. ¹H NMR (CD₂Cl₂, 300 MHz): δ 7.62–7.44 (m, 15H, AuPPh₃), 5.83 (app t, *J* = 2.1 Hz, 2H, Cp), 5.21 (app t, *J* = 2.1 Hz, 2H, Cp), 2.52–2.34 (m, 4H, CH₂CH₂N), 2.11 (s, 6H, CH₃). ¹³C{¹H} NMR (CD₂Cl₂, 75 MHz): δ 231.8 (s, CO), 134.6 (d, ²J_{PC} = 14.6 Hz, *ortho* C, AuPPh₃), 131.8 (d, ⁴J_{PC} = 2.5 Hz, *para* C, AuPPh₃), 131.0 (d, ¹J_{PC} = 50.8 Hz, *ipso* C, AuPPh₃), 129.6 (d, ³J_{PC} = 11.2 Hz, *meta* C, AuPPh₃), 112.1 (s, quaternary C, Cp), 88.2 (s, Cp), 86.8 (s, Cp), 61.9 (s, CH₂CH₂N), 45.9 (s, CH₃), 28.1 (s, CH₂CH₂N).

W(AuPPh₃)(CO)₃(η^5 -Cp^N)(9). Yield: 49%. Anal. Calcd for C₃₀H₂₉AuNO₃PW: C, 41.74; H, 3.39; N, 1.62. Found: C, 41.62; H, 3.34; N, 1.53. Mp: 99–100 °C (dec). IR (DME) ν (CO): 1943

Table 1. Crystal Data, Data Collection, Solution, and Refinement for 1–4

	1	2	3	4
empirical formula	C ₁₂ H ₁₅ CrNO ₃	C ₁₂ H ₁₅ MoNO ₃	C ₁₂ H ₁₅ NO ₃ W	C ₁₂ H ₁₆ ClNO ₃ W
fw	273.25	317.19	405.10	441.56
cryst color	yellow	colorless	colorless	colorless
morphology	pyramid	block	block	plate
cryst size (mm)	0.20 × 0.20 × 0.20	0.22 × 0.20 × 0.08	0.15 × 0.12 × 0.08	0.16 × 0.12 × 0.03
cryst syst	monoclinic	monoclinic	monoclinic	orthorhombic
space group	<i>P</i> 2 ₁ / <i>n</i>	<i>P</i> 2 ₁ / <i>n</i>	<i>P</i> 2 ₁ / <i>n</i>	<i>Pnma</i>
<i>a</i> (Å)	7.0927(8)	7.1688(8)	7.1578(6)	26.028(4)
<i>b</i> (Å)	13.3643(14)	13.5094(14)	13.4710(12)	8.0667(11)
<i>c</i> (Å)	12.5749(13)	12.6905(13)	12.6744(11)	6.9001(10)
α (deg)	90	90	90	90
β (deg)	91.057(2)	93.127(2)	92.8780(10)	90
γ (deg)	90	90	90	90
<i>V</i> (Å ³)	1191.8(2)	1227.2(2)	1220.56(18)	1448.8(4)
<i>Z</i>	4	4	4	4
ρ(calc) (Mg m ⁻³)	1.523	1.717	2.205	2.024
μ (mm ⁻¹)	0.955	1.064	9.459	8.157
<i>F</i> (000)	568	640	768	840
θ range (deg)	2.22–27.51	2.20–27.52	2.21–27.51	1.56–27.49
index ranges	−9 ≤ <i>h</i> ≤ 9 0 ≤ <i>k</i> ≤ 17 0 ≤ <i>l</i> ≤ 16	−9 ≤ <i>h</i> ≤ 9 0 ≤ <i>k</i> ≤ 17 0 ≤ <i>l</i> ≤ 16	−9 ≤ <i>h</i> ≤ 9 0 ≤ <i>k</i> ≤ 17 0 ≤ <i>l</i> ≤ 16	−33 ≤ <i>h</i> ≤ 32 −10 ≤ <i>k</i> ≤ 10 −8 ≤ <i>l</i> ≤ 8
no. of rflns collected	9901	14 940	14 901	13 448
no. of indep rflns	2719	2830	2809	1776
<i>R</i> (int) ^a	0.0261	0.0466	0.0381	0.0685
no. of obsd rflns	2394	2518	2566	1362
max./min. transmn	0.8320/0.8320	0.9197/0.7996	0.5183/0.3311	0.7919/0.3552
no. of data/restraints/params	2719/0/156	2830/0/156	2809/0/156	1776/2/107
<i>R</i> ₁ ^b w <i>R</i> ₂ ^c (<i>I</i> > 2σ(<i>I</i>))	0.0332; 0.0756	0.0224; 0.0567	0.0182; 0.0465	0.0363; 0.0780
GOF on <i>F</i> ²	1.089	1.070	1.074	1.048
largest diff peak/hole (e Å ⁻³)	0.328/−0.346	0.463/−0.266	1.253/−0.462	1.365/−1.703

^a *R*(int) = Σ|*F*_o² − ⟨*F*_c²⟩/Σ|*F*_o²|. ^b *R*₁ = Σ||*F*_o − |*F*_c||/Σ|*F*_o|. ^c w*R*₂ = [Σ[w(*F*_o² − *F*_c²)²]/Σ[w(*F*_o²)²]]^{1/2}.

(s), 1856 (m, sh), 1835 (s) cm⁻¹; (THF) ν(CO): 1943 (s), 1857 (m, sh), 1836 (s) cm⁻¹; (Nujol) ν(CO): 1932 (s), 1818 (s) cm⁻¹. ¹H NMR (CD₂Cl₂, 300 MHz): δ 7.60–7.42 (m, 15H, AuPPh₃), 5.47 (app t, *J* = 2.1 Hz, 2H, Cp), 5.28 (app t, *J* = 2.1 Hz, 2H, Cp), 2.58–2.36 (m, 4H, CH₂CH₂N), 2.11 (s, 6H, CH₃). ¹³C{¹H} NMR (CD₂Cl₂, 75 MHz): δ 221.3 (s, CO, (¹⁸³W–¹³C satellites: 222.42, 220.21, ¹*J*_{WC} = 167 Hz)), 134.6 (d, ²*J*_{PC} = 14.6 Hz, *ortho* C, AuPPh₃), 131.8 (s, *br*, *para* C, AuPPh₃), 129.6 (d, ³*J*_{PC} = 11.2 Hz, *meta* C, AuPPh₃), 110.3 (s, quaternary C, Cp), 87.1 (s, Cp), 85.5 (s, Cp), 61.9 (s, CH₂CH₂N), 45.7 (s, CH₃), 28.0 (s, CH₂CH₂N).

X-ray Crystallographic Characterization of 1–8. X-ray quality crystals of 1–6 were obtained by diffusion of Et₂O into a CH₃CN solution of each compound. Crystals of 7 were obtained by evaporation of an 80% v/v pentane/Et₂O solution. Crystals of 8 were obtained by evaporation of a pentane solution. All manipulations with the crystals of 1–6 were conducted in a N₂-filled glovebag; these crystals were selected from the mother liquor. Crystals of 7 and 8 were dried in vacuo and selected in air. A selected crystal was coated with viscous oil, placed onto the tip of a 0.1 mm diameter glass capillary, and mounted on a Bruker SMART Platform CCD diffractometer for data collection (Mo Kα radiation with λ = 0.71073 Å) at 173(2) K. For 1–5, 7, and 8, a preliminary set of cell constants was calculated from reflections harvested from three sets of 20 frames; four sets of 30 frames were used for 6. The SMART program^{15a} indexed the non-twins 1–5 and 7. The CellNow program^{15b} indexed 6 as a two-component non-merohedral twin; of the 424 reflections used, 303 indexed exclusively to twin component 1, 121 indexed exclusively to twin component 2, and 167 were common to both. The twin law for 6 is best described as an 180° rotation in reciprocal space about the [101] axis. The twin law matrix by rows is [0.233 0.000 −0.766/0.000 −1.000 0.000/−1.234 0.000 −0.233]. The CellNow program^{15b} also indexed 8 as a two-component

non-merohedral twin with twin law [1 0 0/0 −1 0/0.564 0 −1], an 180° rotation about the [100] axis in reciprocal space. Out of 194 reflections, 43 indexed uniquely to component 1, 43 indexed uniquely to component 2, 148 were common to both, and no reflections were left unindexed. During data collection a randomly oriented region of reciprocal space was surveyed to the extent of one sphere to a resolution of 0.77 Å (1–7) or 0.84 Å (8). Four major sections of frames were collected with 0.30° steps in ω. Final cell constants were calculated from the actual data collection after integration (SAINT).^{15a} The intensity data were corrected for absorption and decay by the SADABS¹⁶ (1–5, 7) or TWINABS^{15b,16b} (6, 8) program. The Strip Redundant V13 program^{15c} removed redundant reflections from the data of 8. Reflections involving systematic absences were removed from the data of 8 with the SysAbsFilterV13 program.^{15c} Space groups were determined on the basis of systematic absences and intensity statistics. Successful direct-methods solutions were calculated, which provided most non-hydrogen atoms from the E-maps. Several full-matrix least-squares/difference Fourier cycles were performed to locate the remainder of the non-hydrogen atoms. All non-hydrogen atoms were refined with anisotropic displacement parameters. All hydrogen atoms, except the hydride of 4, were placed in ideal positions and refined as riding atoms with relative isotropic displacement parameters. The tungsten hydride of 4 was found from the difference map and refined accordingly. For 3, the largest difference Fourier peak is in the vicinity of the W atom. The unit cell of 8 features a small void (34 Å³) that water may occupy; there is no peak in the difference Fourier to suggest any solvent. For 8, the ratio of twin components is 0.606:0.394. All calculations were performed on Pentium computers using the SHELXTL V6.14 suite of programs.^{15a} Crystal data, data collection, solution, and refinement information for 1–4 and 5–8 are provided in Tables 1 and 2, respectively.

(15) (a) SMART V5.054 2001, SAINT+ V6.45 2003, SHELXTL V6.14 2000; Bruker Analytical X-ray Systems: Madison, WI. (b) CellNow, TWINABS; G. M. Sheldrick, 2003. (c) Strip Redundant V13, SysAbsFilterV13; W. W. Brennessel, V. G. Young, Jr., 2003, unpublished programs.

(16) (a) SADABS (Siemens Area Detector Absorption correction program); G. M. Sheldrick, 1996. (b) Blessing, R. *Acta Crystallogr.* 1995, A51, 33.

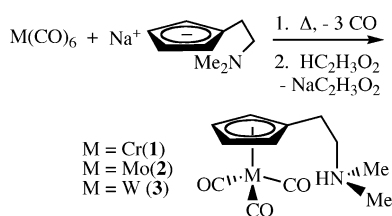
Table 2. Crystal Data, Data Collection, Solution, and Refinement for 5–8

	5	6	7	8
empirical formula	C ₃₀ H ₃₀ AuClMoNO ₃ P	C ₃₀ H ₃₀ AuClNO ₃ PW	C ₃₀ H ₂₉ AuCrNO ₃ P	C ₃₀ H ₂₉ AuMoNO ₃ P
fw	811.88	899.79	731.48	775.42
cryst color	colorless	colorless	colorless	colorless
morphology	needle	needle	needle	needle
cryst size (mm)	0.13 × 0.07 × 0.06	0.30 × 0.10 × 0.08	0.40 × 0.05 × 0.05	0.35 × 0.05 × 0.04
cryst syst	monoclinic	monoclinic	monoclinic	monoclinic
space group	<i>P</i> 2 ₁ / <i>n</i>	<i>P</i> 2 ₁ / <i>c</i>	<i>P</i> 2 ₁ / <i>c</i>	<i>P</i> 2 ₁ / <i>c</i>
<i>a</i> (Å)	8.9559(9)	15.541(2)	11.169(4)	11.8991(16)
<i>b</i> (Å)	23.828(2)	23.874(3)	19.417(8)	18.567(3)
<i>c</i> (Å)	14.0808(14)	17.795(3)	13.637(5)	13.8647(19)
α (deg)	90	90	90	90
β (deg)	97.029(2)	115.381(2)	106.889(6)	109.127(2)
γ (deg)	90	90	90	90
<i>V</i> (Å ³)	2982.3(5)	5965.1(15)	2829.9(19)	2894.1(7)
<i>Z</i>	4	8	4	4
ρ (calc) (Mg m ⁻³)	1.808	2.004	1.717	1.780
μ (mm ⁻¹)	5.508	8.941	5.650	5.582
<i>F</i> (000)	1576	3408	1432	1504
θ range (deg)	1.69–27.51	1.45–27.53	1.88–27.49	1.81–25.03
index ranges	–11 ≤ <i>h</i> ≤ 11 0 ≤ <i>k</i> ≤ 30 0 ≤ <i>l</i> ≤ 18	–20 ≤ <i>h</i> ≤ 18 0 ≤ <i>k</i> ≤ 31 0 ≤ <i>l</i> ≤ 23	–14 ≤ <i>h</i> ≤ 14 –25 ≤ <i>k</i> ≤ 24 –17 ≤ <i>l</i> ≤ 16	–14 ≤ <i>h</i> ≤ 13 0 ≤ <i>k</i> ≤ 22 0 ≤ <i>l</i> ≤ 16
no. of rflns collected	35 927	117 682	25 554	46 807
no. of indep rflns	6850	13 682	6456	5113
<i>R</i> (int) ^a	0.0596	0.0900	0.0584	0.0760
no. of obsd rflns	5221	10158	4593	3941
Max./min. transmn	0.7334/0.5345	0.5348/0.1745	0.7654/0.2109	0.8076/0.2454
no. of data/restraints/params	6850/0/345	13 682/0/690	6456/0/336	5113/0/337
R1, ^b wR2 ^c (<i>I</i> > 2 σ (<i>I</i>))	0.0350; 0.0728	0.0328; 0.0584	0.0394; 0.0682	0.0318; 0.0441
GOF on <i>F</i> ²	1.106	0.990	1.039	0.995
largest diff peak/hole (e Å ⁻³)	1.809/–0.627	1.501/–0.972	0.824/–1.429	1.084/–0.785

^a $R(\text{int}) = \sum |F_o^2 - \langle F_c^2 \rangle| / \sum |F_o^2|$. ^b $R1 = \sum ||F_o| - |F_c|| / \sum |F_o|$. ^c $wR2 = [\sum [w(F_o^2 - F_c^2)^2] / \sum [w(F_o^2)^2]]^{1/2}$.

Table 3. $\nu(\text{CO})$ IR Data (cm⁻¹) for M(CO)₃(η^5 -Cp^{NH}) and [PPN][M(CO)₃(η^5 -Cp^N)]

complex	CH ₃ CN	THF
1	1906 (s), 1805 (m), 1782 (s)	1910 (s), 1814 (s), 1784 (s)
[PPN][Cr(CO) ₃ (η^5 -Cp ^N)] (10)	1889 (s), 1771 (s)	1890 (m), 1776 (s)
2	1911 (s), 1809 (s), 1788 (s)	1915 (s), 1819 (s), 1790 (s)
[PPN][Mo(CO) ₃ (η^5 -Cp ^N)] (11)	1893 (s), 1775 (s)	1894 (s), 1779 (s)
3	1904 (s), 1803 (s), 1782 (s)	2015 (m), 1920 (s), 1909 (s), 1813 (s), 1785 (s)
[PPN][W(CO) ₃ (η^5 -Cp ^N)] (12)	1887 (s), 1770 (s)	1888 (s), 1774 (s)

Scheme 1**Results and Discussion**

Synthesis of M(CO)₃(η^5 -Cp^{NH}) and Characterization in Solution. Reactions of M(CO)₆ and NaCp^{NH} followed by protonation with acetic acid afforded M(CO)₃(η^5 -Cp^{NH}) (Scheme 1). These zwitterions engage in tight ion-pairing; the positive charge is completely localized at the ammonium nitrogen and the tethered substituent is sufficiently flexible to permit its approach toward the anionic metal center. Comparison of the $\nu(\text{CO})$ IR spectra of **1–3** with those of [PPN][M(CO)₃(η^5 -Cp^N)]¹⁰ indicates that the M(CO)₃ units of **1–3** are significantly perturbed in solution (Table 3). The perturbation in CH₃CN is noteworthy since alkali metal salts of [M(CO)₃(η^5 -Cp)]⁻ display spectra indicative of a symmetrical solvent field about the anions in this solvent but engage in ion-pairing in THF.¹⁷ The infrared spectra for **1–3**

suggest cation penetration into the coordination sphere, giving C_s ion pairs with reduced electron density at the metal center relative to **10–12**. The lowest and highest energy $\nu(\text{CO})$ absorptions of **1–3** are shifted higher by approximately 12 and 16 cm⁻¹, respectively, relative to the corresponding absorptions of **10–12**. This contrasts the $\nu(\text{CO})$ IR spectra of [NMe₄][M'(CO)₃(η^5 -Cp)] (M' = Cr, Mo) in THF, which suggest contact ion-pairing between the cation and CO ligands.¹⁷ The $\nu(\text{CO})$ IR spectrum of **3** in THF suggests that a second, even tighter ion-pair persists in this solvent. Although the additional carbonyl absorptions are strikingly similar to those of WH(CO)₃(η^5 -Cp)¹¹ and **4**, no spectroscopic evidence could be obtained to support proton transfer to tungsten in THF, consistent with the stability of [Et₃NH][W(CO)₃(η^5 -Cp)].¹¹ Tight ion-pairing is also evident in hydrogen-bonding solvents. Complexes **1–3** are sparingly soluble in methanol and pyridine; the $\nu(\text{CO})$ IR spectra in these solvents are similar to those in CH₃CN. The $\nu(\text{CO})$ IR spectra of **1–3** in THF do not change upon addition of excess acetic acid (3 equiv). The δ ¹³-CO of **1–3** in CD₃CN are upfield those of **10–12** in this solvent by 2.9, 3.3, and 3.5 ppm, respectively (Table 4). These chemical shifts for **1–3** are solvent dependent; the ¹³CO resonances of **1**, **2**, and **3** in CD₂Cl₂ are shifted upfield 1.0, 1.4, and 3.6 ppm, respectively, relative to those in CD₃CN. The $\nu(\text{CO})$ IR and ¹³CO NMR spectral data suggest that **3** exhibits the tightest ion-pairing

(17) Darensbourg, M. Y.; Jimenez, P.; Sackett, J. R.; Hanckel, J. M.; Kump, R. L. *J. Am. Chem. Soc.* **1982**, *104*, 1521.

Table 4. ^{13}C NMR ^{13}CO Chemical Shifts (ppm) of $\text{M}(\text{CO})_3(\eta^5\text{-Cp}^{\text{NH}})$ and $[\text{PPN}][\text{M}(\text{CO})_3(\eta^5\text{-Cp}^{\text{N}})]$

complex	CD_3CN	$\text{C}_4\text{D}_8\text{O}$	CD_2Cl_2
1	244.1	243.3	243.1
10	247.0		
2	234.0	232.9	232.6
11	237.3		
3	224.6	221.4	221.0
12	228.1		

among these zwitterions. This is consistent with $[\text{W}(\text{CO})_3(\eta^5\text{-Cp})]^-$ being the most basic among its group VI analogues.

The possibility that $\text{N-H}\cdots\text{M}$ hydrogen bonds accompany the tight ion-pairing of **1–3** in solution cannot be ruled out. Downfield shifts of the ^1H NMR bridging hydrogen atom resonance are diagnostic of hydrogen bonding. The δ NH of **1–3** is solvent and concentration dependent; the limited solubility of **2** and **3** permitted evaluation of only dilute solutions of these complexes (Table 5). The ammonium hydrogen of $[\text{Et}_3\text{NH}][\text{Co}(\text{CO})_4]$ exhibits a resonance at δ 8.31 in C_6D_6 .¹⁸ In $\text{Mo}(\text{PMe}_3)_3(\eta^6\text{-C}_6\text{H}_5\text{C}_6\text{H}_3(\text{Ph})\text{OH})$ (**13**), the bridging hydroxylic hydrogen is coupled to the three phosphorus nuclei and exhibits a resonance at δ 8.2.⁸ Deshielding of the bridging hydrogen as solute concentration increases is a general condition associated with hydrogen bonding. The concentration dependence of δ NH appears to be independent of solution composition; a CD_3CN solution containing equimolar quantities of **1–3** (total conc 0.165 M) exhibited a single NH resonance at δ 9.81, nearly identical to that of a 0.17 M solution of **1**. Further NH deshielding as solvent polarity decreases ($\text{C}_4\text{D}_8\text{O}$, $\text{CD}_2\text{-Cl}_2$) is consistent with enhanced hydrogen bonding due to even tighter ion-pairing.

Structural Characterization of $\text{M}(\text{CO})_3(\eta^5\text{-Cp}^{\text{NH}})$.

Complexes **1–3** were characterized by single-crystal X-ray crystallography to examine the ion-pairing interaction in the solid state. The three-legged piano-stool structures of **1–3** are shown in Figures 1–3, respectively. The $\text{N}\cdots\text{M}$ distances 3.5479(15), 3.6068(16), and 3.613(2) Å in **1–3**, respectively, are similar to the $\text{O}\cdots\text{Mo}$ separation in **13** (3.571(2) Å)⁸ and the intermolecular $\text{N}\cdots\text{Co}$ length of $[\text{Et}_3\text{NH}][\text{Co}(\text{CO})_4]$ (3.667(2) Å),¹⁸ consistent with hydrogen bonding in the solid state. The NH hydrogen atoms of **1–3** were not located, so $\text{H}\cdots\text{M}$ lengths and N-H-M angles for **1–3** were calculated (Supporting Information) on the basis of the N-H length (1.033 Å) expected from neutron diffraction.¹⁹ Although these calculated parameters are also consistent with hydrogen-bonding interactions involving transition metal acceptors, the elongated neutron diffraction N-H distance in $[\text{Et}_3\text{NH}][\text{Co}(\text{CO})_4]$ (1.054(1) Å)¹⁸ indicates that accurate determination of NH hydrogen coordinates is required to unambiguously characterize these intramolecular interactions as hydrogen bonds.

The electrostatic attraction between the anionic metal centers and the ammonium ion results in marked structural differences in **1–3** relative to their conjugate bases **10–12**.¹⁰ Approach of the pendant cation toward $\text{M}(\text{CO})_3$ units causes widening of $\text{C}(12)\text{-M-C}(10)$ ac-

companied by significant irregularity in the $(\text{O})\text{C-M-C}(\text{O})$ angles of **1–3**. The $\text{C}(12)\text{-M-C}(10)$ angles are larger than the corresponding $\text{C}(12)\text{-M-C}(11)$ angles by approximately 7.5° , 6.8° , and 6.6° in **1–3**, respectively. Compression of $\text{C}(12)\text{-M-C}(11)$ primarily accommodates $\text{C}(12)\text{-M-C}(10)$ expansion; the $\text{M}(10)\text{-M-C}(11)$ angles of **1–3** are statistically indistinguishable from the average $(\text{O})\text{C-M-C}(\text{O})$ angles of **10–12**, respectively. Important average structural parameters for the $\text{M}(\text{CO})_3$ units of **1–3** (**1**: $\text{Cr-C}(\text{O})$, 1.820(7) Å; C-O , 1.169(6) Å; O-C-Cr , $178.2(5)^\circ$; **2**: $\text{Mo-C}(\text{O})$, 1.946(11) Å; C-O , 1.16(1) Å; O-C-Mo , $177.8(9)^\circ$; **3**: $\text{W-C}(\text{O})$, 1.944(9) Å; C-O , 1.171(8) Å; O-C-W , $177.2(9)^\circ$) are statistically identical to those of **10–12**, respectively. However, the slight elongation of average $\text{M-C}(\text{O})$ lengths ($\sim 1-2\sigma$) and contraction of average C-O lengths ($\sim 1\sigma$) in **1–3** are consistent with less electron rich metal centers than found in **10–12**. Although the average $\text{M-C}(\text{dienyl})$ lengths of **1–3** (**1**, 2.217(5) Å; **2**, 2.379(4) Å; **3**, 2.367(5) Å) are statistically indistinguishable from those of **10–12**, the minor ring slippage in **10–12**, attributed to steric hindrance between the 2-(dimethylamino)ethyl substituent and $\text{M}(\text{CO})_3$ fragment, is not observed in the unambiguously $\eta^5\text{-Cp}$ complexes **1–3**. The approach of the pendant cation toward $\text{M}(\text{CO})_3$ draws $\text{C}(1)$ closer to the metal and results in nearly uniform $\text{M-C}(\text{dienyl})$ lengths.

Protonation of $\text{M}(\text{CO})_3(\eta^5\text{-Cp}^{\text{NH}})$. The Brønsted basicity of the formally anionic metal centers of **1–3** is reduced relative to that of $[\text{M}(\text{CO})_3(\eta^5\text{-Cp})]^-$. Addition of excess acetic acid to **1–3** did not protonate the metal centers of these zwitterions even though this acid reacts with $\text{Na}[\text{M}(\text{CO})_3(\eta^5\text{-Cp})]$ to provide $\text{MH}(\text{CO})_3(\eta^5\text{-Cp})$.²⁰ While strong acids stoichiometrically react with $[\text{M}(\text{CO})_3(\eta^5\text{-Cp})]^-$ to provide these hydrides, attempts to isolate pure salts containing $[\text{M}'\text{H}(\text{CO})_3(\eta^5\text{-Cp}^{\text{NH}})]^+$ ($\text{M}' = \text{Cr}, \text{Mo}$) were uniformly unsuccessful. Reactions of **1** and **2** with 1 equiv of phosphoric acid, concentrated hydrochloric acid, or trifluoroacetic acid in THF resulted in a mixture of metal hydride and starting zwitterion on the basis of IR spectroscopy; the product $\nu(\text{CO})$ absorptions were very similar to those of $\text{M}'\text{H}(\text{CO})_3(\eta^5\text{-Cp})$.¹¹ Excess strong acid (5–10 equiv) was required to completely protonate **1** and **2** in solution. However, attempts to isolate the metal hydride products, with removal of the excess acid, resulted in formation of **1** and **2**. Protonation of **1** with these acids in CH_3CN provided the same outcome. Reaction of **2** with 1 equiv of these acids in CH_3CN at -10°C resulted in instantaneous production of $\text{Mo}(\text{CO})_3(\text{CH}_3\text{CN})_3$ via reductive elimination. The hydride $\text{MoH}(\text{CO})_3(\eta^5\text{-Cp})$ decomposes in acetonitrile to provide $\text{Mo}(\text{CO})_3(\text{CH}_3\text{CN})_3$, but the reaction was found sufficiently slow at 0°C to permit experimentation with the hydride at that temperature.^{11,21} Pure $[\text{WH}(\text{CO})_3(\eta^5\text{-Cp}^{\text{NH}})]\text{Cl}$ (**4**) was obtained from the reaction of **3** and hydrochloric acid (Scheme 2). The lower and higher energy $\nu(\text{CO})$ absorptions of **4** in CH_3CN are shifted higher by 8 and 11 cm^{-1} , respectively, relative to those of $\text{WH}(\text{CO})_3(\eta^5\text{-Cp})$ (**14**) in CH_3CN .¹¹ A ^1H NMR resonance at $\delta -7.25$ for the tungsten hydride of **4** in $\text{CD}_3\text{-}$

(18) Brammer, L.; McCann, M. C.; Morris Bullock, R.; McMullan, R. K.; Sherwood, P. *Organometallics* **1992**, *11*, 2339.

(19) *International Tables for Crystallography*; Kluwer: Dordrecht, 1992; Vol. C, Table 9.5.1.1, p 703.

(20) Haines, R. J.; Nyholm, R. S.; Stiddard, M. H. B. *J. Chem. Soc. (A)* **1968**, 46.

(21) Kubas, G. J.; Kiss, G.; Hoff, C. D. *Organometallics* **1991**, *10*, 2870.

Table 5. ^1H NMR NH Chemical Shifts (ppm) of $\text{M}(\text{CO})_3(\eta^5\text{-Cp}^{\text{NH}})$

	solvent								
	CD_3CN	CD_3CN	CD_3CN	CD_3CN	CD_3CN	CD_3CN	CD_3CN	$\text{C}_4\text{D}_8\text{O}$	CD_2Cl_2
conc (M)	0.067	0.10	0.13	0.17	0.20	0.27	sat.	sat.	sat.
1	8.46	8.92	9.41	9.78	10.07	10.27	10.34 ^a	11.79 ^d	12.15 ^f
2	8.02	8.68	9.15				9.20 ^b	11.48 ^e	11.90 ^g
3	7.83	8.40					8.80 ^c	<i>h</i>	<i>h</i>

Sat. conc (M): ^a 0.29. ^b 0.15. ^c 0.12. ^d 0.07. ^e 0.05. ^f 0.06. ^g 0.04. ^h Resonance not observed.

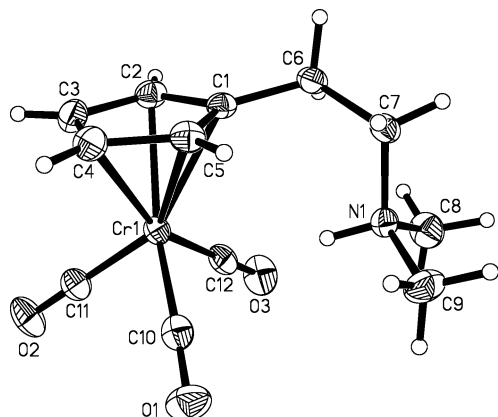


Figure 1. Molecular structure of **1** (50% thermal ellipsoids). Selected bond lengths (Å) and angles (deg): Cr–C(1) = 2.2224(17), Cr–C(2) = 2.2111(18), Cr–C(3) = 2.214(2), Cr–C(4) = 2.2203(19), Cr–C(5) = 2.2184(17), Cr–C(10) = 1.8239(19), Cr–C(11) = 1.8238(19), Cr–C(12) = 1.8122(19), C(10)–O(1) = 1.167(2), C(11)–O(2) = 1.165(2), C(12)–O(3) = 1.176(2), C(12)–Cr–C(10) = 93.47(8), C(12)–Cr–C(11) = 85.96(8), C(10)–Cr–C(11) = 88.43(8), O(1)–C(10)–Cr = 177.90(17), O(2)–C(11)–Cr = 178.75(16), O(3)–C(12)–Cr = 178.00(18).

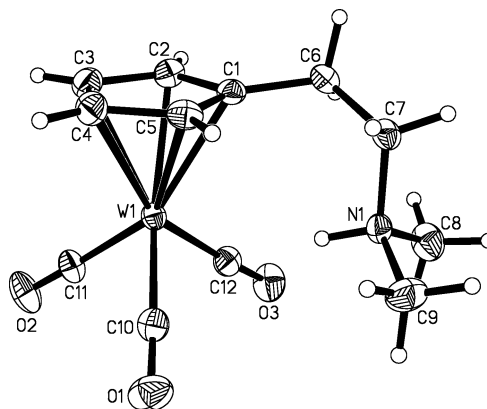


Figure 3. Molecular structure of **3** (50% thermal ellipsoids). Selected bond lengths (Å) and angles (deg): W–C(1) = 2.374(3), W–C(2) = 2.365(3), W–C(3) = 2.361(3), W–C(4) = 2.372(3), W–C(5) = 2.365(3), W–C(10) = 1.948(3), W–C(11) = 1.950(3), W–C(12) = 1.934(3), C(10)–O(1) = 1.167(4), C(11)–O(2) = 1.165(4), C(12)–O(3) = 1.180(4), C(12)–W–C(10) = 91.26(13), C(12)–W–C(11) = 84.70(13), C(10)–W–C(11) = 86.74(13), O(1)–C(10)–W = 176.6(3), O(2)–C(11)–W = 178.3(3), O(3)–C(12)–W = 176.8(3).

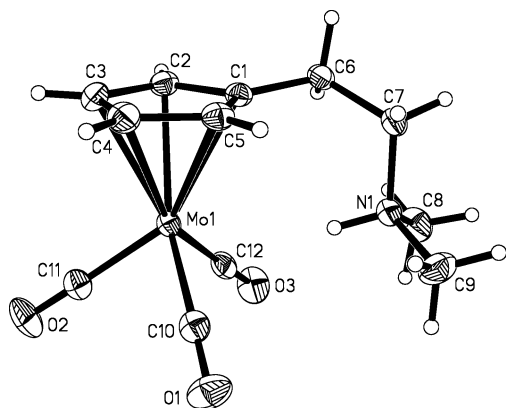
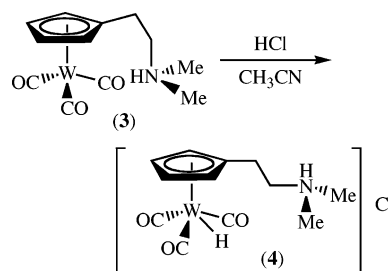


Figure 2. Molecular structure of **2** (50% thermal ellipsoids). Selected bond lengths (Å) and angles (deg): Mo–C(1) = 2.3833(18), Mo–C(2) = 2.3744(19), Mo–C(3) = 2.377(2), Mo–C(4) = 2.3833(19), Mo–C(5) = 2.3752(19), Mo–C(10) = 1.945(2), Mo–C(11) = 1.958(2), Mo–C(12) = 1.936(2), C(10)–O(1) = 1.166(2), C(11)–O(2) = 1.154(2), C(12)–O(3) = 1.174(2), C(12)–Mo–C(10) = 91.05(8), C(12)–Mo–C(11) = 84.21(8), C(10)–Mo–C(11) = 86.36(8), O(1)–C(10)–Mo = 177.26(17), O(2)–C(11)–Mo = 178.78(18), O(3)–C(12)–Mo = 177.22(18).

CN is intermediate that of **14** (δ –7.40)¹¹ and $\text{WH}(\text{CO})_3(\eta^5\text{-C}_5\text{H}_4\text{CO}_2\text{H})$ (**15**) (δ –7.03)²² in this solvent.

Structural Characterization of $[\text{WH}(\text{CO})_3(\eta^5\text{-Cp}^{\text{NH}})]\text{Cl}$. Complex **4** was characterized by single-crystal X-ray crystallography, and its molecular structure is

Scheme 2

shown in Figure 4. Complex **4** lies on a crystallographic mirror plane. Four pendant group atoms (C(4–7)) are disordered 50:50 over this plane. The related $\text{MoH}(\text{CO})_3(\eta^5\text{-Cp})$ (**16**) also adopts an approximate C_s molecular symmetry.²³ The configuration of **4**, in which the carbonyl trans to the hydride is staggered with respect to C–H bonds of the Cp ring, while the hydride and two carbonyl ligands are oriented in a nearly eclipsed orientation, is consistent with the structures of **15**²² and **16**. It is noteworthy that the hydride of **4** was located and refined since this was not possible with **14**²⁴ and **15**, previous $\text{WH}(\text{CO})_3(\eta^5\text{-C}_5\text{H}_x\text{R}_{5-x})$ complexes characterized by X-ray crystallography. The W–H distance of **4** is statistically indistinguishable from that determined for gas phase **14** (1.79(2) Å) (microwave spectroscopy)²⁵ and the Mo–H distance in $\text{MoH}(\text{CO})_3(\eta^5\text{-C}_5\text{Me}_5)$ (1.789(7) Å) (neutron diffraction).²³ In **4**, the $\eta^5\text{-Cp}$ ring is

(22) Shafiq, F.; Szalda, D. J.; Creutz, C.; Morris Bullock, R. *Organometallics* **2000**, *19*, 824.

(23) Brammer, L.; Zhao, D.; Morris Bullock, R.; McMullan, R. K. *Inorg. Chem.* **1993**, *32*, 4819.

(24) Johnson, P. L. *Diss. Abstr. B* **1968**, *2905*, 1626.

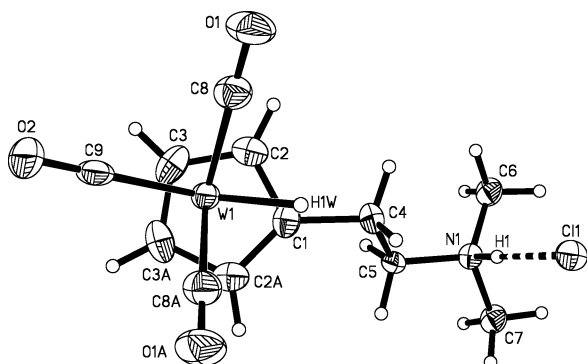


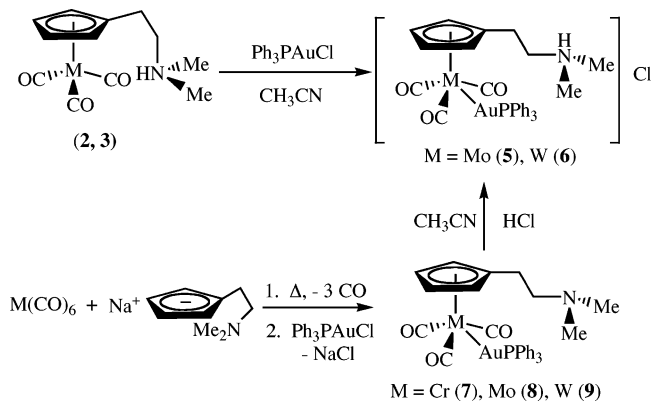
Figure 4. Molecular structure of **4** (50% thermal ellipsoids). Selected bond lengths (Å) and angles (deg): W–H(1W) = 1.75(9), W–C(1) = 2.373(9), W–C(2) = 2.345(6), W–C(2A) = 2.346(6), W–C(3/3A) = 2.306(7), W–C(8/8A) = 1.971(7), W–C(9) = 1.969(10), C(8/8A)–O(1/1A) = 1.147(8), C(9)–O(2) = 1.173(12), N···Cl = 3.066(7), C(8A)–W–C(8) = 106.5(4), C(9)–W–C(8/8A) = 80.6(3), O(1/1A)–C(8/8A)–W = 178.3(7), O(2)–C(9)–W = 178.0(10).

oriented such that the tethered group occupies space above the hydride and between symmetrically equivalent CO ligands defined by C(8) and C(8A). In **15**, the carboxylic acid function and the assumed location of the hydride are between different sets of carbonyl ligands. The impact of Cp substituent orientation on the (O)C–W–C(O) angle that accommodates the hydride appears minimal, as this angle in **4** (106.5(4)°) is only slightly larger than that of **15** (105.1(4)°). Important average structural parameters of **4** (W–C(O), 1.970(1) Å; W–C(dienyl), 2.34(3) Å; C–O, 1.16(2) Å; O–C–W, 178.2(2)°) are statistically identical to those of **15**. However, the W–C(O) distances of **4** are significantly more uniform than in **15** (av 1.96(2) Å), where the carbonyl trans to the hydride has the longest W–C(O) length. The η^5 -Cp of **4** engages in minor tilting; the W–C(1) distance is 0.067 Å longer ($\sim 7\sigma$) than the uniform W–C(3/3A) distances due to steric influence of the substituent.

Reactions of $M(\text{CO})_3(\eta^5\text{-Cp}^{\text{NH}})$ with Triphenylphosphinegold(I) Chloride. An investigation into the metal-based nucleophilicity of **1–3** was initiated with reactions of the zwitterions and Ph_3PAuCl due to the $\text{AuPPh}_3^+/\text{H}^+$ isolobal analogy. Reactions of **1** and Ph_3PAuCl in THF and CH_3CN were reminiscent of the unsuccessful protonation attempts of **1**. Excess Ph_3PAuCl (3 equiv) was required to completely convert **1** to $[\text{Cr}(\text{AuPPh}_3)(\text{CO})_3(\eta^5\text{-Cp}^{\text{NH}})]\text{Cl}$ in solution on the basis of IR spectroscopy; its $\nu(\text{CO})$ IR spectrum was nearly identical with that of $\text{Cr}(\text{AuPPh}_3)(\text{CO})_3(\eta^5\text{-Cp}^{\text{N}})$ (**7**). Subsequent removal of excess Ph_3PAuCl resulted in formation of **1**; pure samples of $[\text{Cr}(\text{AuPPh}_3)(\text{CO})_3(\eta^5\text{-Cp}^{\text{NH}})]\text{Cl}$ could not be obtained. Pure salts $[\text{M}(\text{AuPPh}_3)(\text{CO})_3(\eta^5\text{-Cp}^{\text{NH}})]\text{Cl}$ (M = Mo (**5**), W (**6**)) were isolated from reactions of **2** and **3**, respectively, with Ph_3PAuCl . Complexes **5** and **6** were also accessible via protonation of $\text{M}(\text{AuPPh}_3)(\text{CO})_3(\eta^5\text{-Cp}^{\text{N}})$ (M = Mo (**8**), W (**9**)) with concentrated HCl (1 equiv). Reactions of $\text{M}(\text{CO})_6$ and NaCp^{N} , followed by addition of Ph_3PAuCl , afforded complexes **7–9** (Scheme 3). Concentrated HCl (1 equiv) reacted with **7** to provide **1**.

(25) (a) Tanjaroon, C.; Karunatilaka, C.; Keck, K. S.; Kukolich, S. G. *Organometallics* **2005**, *24*, 2848. (b) Tanjaroon, C.; Keck, K. S.; Sebonia, M. M.; Karunatilaka, C.; Kukolich, S. G. *J. Chem. Phys.* **2004**, *121*, 1449.

Scheme 3



Characterization of $\text{Cr}(\text{AuPPh}_3)(\text{CO})_3(\eta^5\text{-Cp}^{\text{N}})$. The spectroscopic data for **7** are consistent with Cp^{N} being the strongest donor ligand among related $\text{Cr}(\text{AuPPh}_3)(\text{CO})_3(\eta^5\text{-C}_5\text{H}_x\text{R}_{5-x})$ complexes. The $\nu(\text{CO})$ IR absorptions of **7** are shifted to lower energies than the corresponding absorptions of $\text{Cr}(\text{AuPPh}_3)(\text{CO})_3(\eta^5\text{-Cp})$,²⁰ $\text{Cr}(\text{AuPPh}_3)(\text{CO})_3(\eta^5\text{-C}_5\text{H}_4\text{CHO})$ (**17**),²⁶ and $[(\text{CO})_3\text{Cr}(\mu, \eta^5\text{-C}_5\text{H}_4\text{PPh}_2)\text{Au}]_2$,²⁷ the $\delta^{13}\text{CO}$ of **7** (240.2) is also downfield that of **17** (δ 236.6). Although AuPR_3 ligands are ubiquitous, **7** is only the fourth complex containing a Cr–AuPR₃ unit to be characterized by X-ray crystallography and the second containing a structurally characterized unsupported bond of this type. The four-legged piano-stool structure of **7** is displayed in Figure 5. The Au–Cr length of **7** (2.6291(11) Å) is statistically identical to those of **17** (2.632(2) Å)²⁶ and $[\text{n-Bu}_4\text{N}][\text{Au}(\text{Cr}(\text{CO})_3(\eta^5\text{-Cp}))_2]$ (2.641(9), 2.635(8) Å)²⁸ and shorter than the supported Au–Cr bonds in $(\text{Ph}_3\text{PAu})(\mu\text{-H})\text{Cr}(\text{CO})_5$ (2.770(2) Å)²⁹ and *cis*- $\{\eta^2\text{-(Ph}_3\text{PAu)}_2\}\text{Cr}(\text{CO})_4(\text{PPh}_3)$ (2.7038(7), 2.6932(6) Å).³⁰ Important average structural parameters of **7** (Cr–C(O), 1.84(1) Å; C–O, 1.168(9) Å; M–C(dienyl), 2.19(1) Å) and the angles that define its $\text{AuCr}(\text{CO})_3$ geometry are statistically indistinguishable from those of **17**. Semibridging carbonyl–gold interactions were claimed in **17** on the basis of the distances between Au and its adjacent CO carbons (2.429(13), 2.494(15) Å) and modest deviation from linearity in the O–C–Cr angles for these ligands (171.3(12)°, 171.8(12)°). Although **7** exhibits nearly identical structural features, other expected changes in the bridging CO ligands associated with this type of interaction are imperceptible and emphasize that these alleged interactions are exceedingly weak. Specifically, elongation in C–O lengths for the semibridging carbonyls relative to the trans C–O distance is statistically indistinguishable. Structural parameters associated with the Au atom and the closer CO defined by C(10) in **7** are very similar to those in $\text{Mo}(\text{AuPPh}_3)(\text{CO})_3(\eta^5\text{-C}_{10}\text{H}_9\text{BNiPr}_2)$ (**18**) (Au–C(O), 2.485(3) Å; C–O, 1.171-

(26) Edelmann, F.; Töfke, S.; Behrens, U. *J. Organomet. Chem.* **1986**, *309*, 87.

(27) Brumas-Soula, B.; Dahan, F.; Poilblanc, R. *New J. Chem.* **1998**, 1067.

(28) Braunstein, P.; Schubert, U.; Burgard, M. *Inorg. Chem.* **1984**, *23*, 4057.

(29) Green, M.; Orpen, A. G.; Salter, I. D.; Stone, F. G. A. *J. Chem. Soc., Chem. Commun.* **1982**, 813.

(30) Esterhuysen, M. W.; Raubenheimer, H. G. *Acta Crystallogr.* **2003**, *C59*, m286.

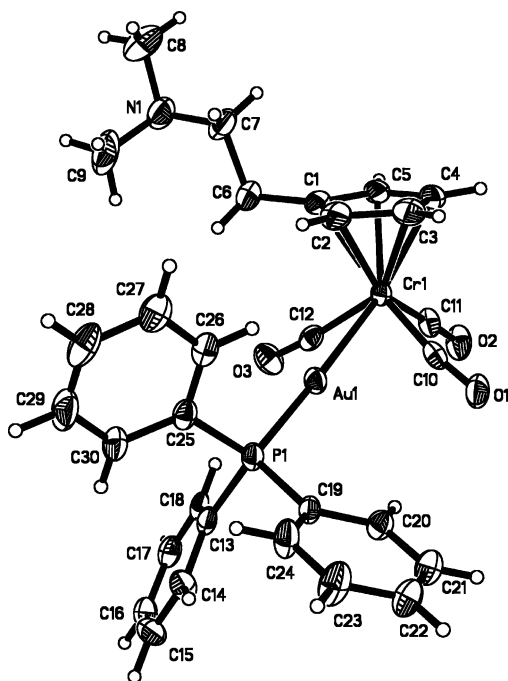


Figure 5. Molecular structure of **7** (50% thermal ellipsoids). Selected bond lengths (Å) and angles (deg): Au–Cr = 2.6291(11), Au–C(10) = 2.461(5), Au–C(12) = 2.493(5), Cr–C(1) = 2.217(5), Cr–C(2) = 2.193(5), Cr–C(3) = 2.184(5), Cr–C(4) = 2.179(5), Cr–C(5) = 2.192(5), Cr–C(10) = 1.841(6), Cr–C(11) = 1.821(5), Cr–C(12) = 1.848(6), O(1)–C(10) = 1.176(6), O(2)–C(11) = 1.159(6), O(3)–C(12) = 1.168(6), P–Au–Cr = 177.59(4), C(10)–Cr–C(12) = 109.3(2), C(10)–Cr–C(11) = 82.0(2), C(11)–Cr–C(12) = 85.9(2), C(11)–Cr–Au = 121.31(17), C(10)–Cr–Au = 63.99(16), C(12)–Cr–Au = 64.98(16), O(1)–C(10)–Cr = 172.1(4), O(2)–C(11)–Cr = 177.2(5), O(3)–C(12)–Cr = 171.9(5).

Table 6. $\nu(\text{CO})$ IR and ^{13}C O NMR Data of $[\text{M}(\text{AuPPh}_3)(\text{CO})_3(\eta^5\text{-Cp}^{\text{NH}})]\text{Cl}$ and $\text{M}(\text{AuPPh}_3)(\text{CO})_3(\eta^5\text{-Cp}^{\text{N}})$ (M = Mo, W)

complex	$\nu(\text{CO})$ IR (cm^{-1})	δ ^{13}C O (ppm)
5	1947 (s), 1910 (vw), 1857 (m, sh), 1837 (s) ^a	232.2 ^b
8	1947 (s), 1862 (m, sh), 1840 (s) ^c	231.8 ^d
6	1943 (s), 1850 (m, sh), 1831 (s) ^a	221.8 ^b
9	1943 (s), 1857 (m, sh), 1836 (s) ^c	221.3 ^d

^a CH₃CN. ^b CD₃CN. ^c THF. ^d CD₂Cl₂

(3) Å; O–C–Mo, 171.5(2)°, where a semibridging interaction was ruled out.³¹

Characterization of $[\text{M}(\text{AuPPh}_3)(\text{CO})_3(\eta^5\text{-Cp}^{\text{NH}})]\text{-Cl}$ and $\text{M}(\text{AuPPh}_3)(\text{CO})_3(\eta^5\text{-Cp}^{\text{N}})$ (M = Mo, W). The $\nu(\text{CO})$ IR and ^{13}C O NMR spectral data of **5**, **8** and **6**, **9**, respectively, are virtually identical (Table 6); protonation of the pendant amine has no apparent electronic impact on the $\text{M}(\text{CO})_3$ units of these complexes. The $\nu(\text{CO})$ IR absorptions of **5** and **8** are shifted to slightly lower energies than those of $\text{Mo}(\text{AuPPh}_3)(\text{CO})_3(\eta^5\text{-Cp})$ (**19**),²⁰ $\text{Mo}(\text{AuPPh}_3)(\text{CO})_3(\eta^5\text{-C}_5\text{H}_4\text{CHO})$ (**20**),³² and $[(\text{CO})_3\text{-Mo}(\eta^5\text{-C}_5\text{H}_4\text{PPh}_2)\text{Au}]_2$.²⁷ These absorptions of **6** and **9** are similarly shifted lower than those of $\text{W}(\text{AuPPh}_3)\text{-}$

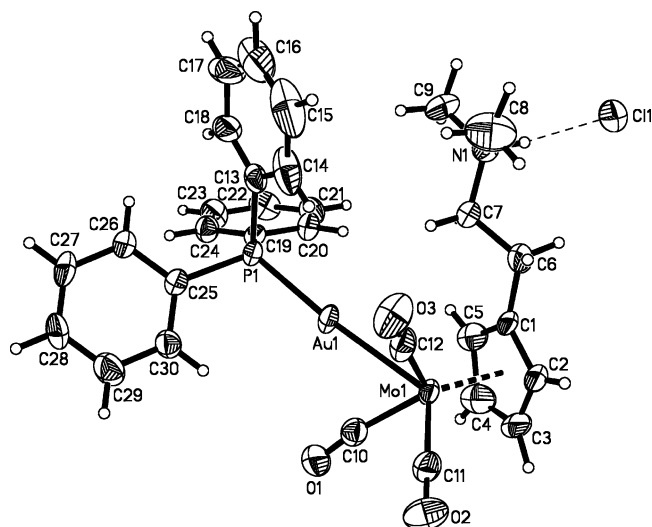


Figure 6. Molecular structure of **5** (50% thermal ellipsoids). Selected bond lengths (Å) and angles (deg): Au–Mo = 2.7063(5), Au–C(10) = 2.540(6), Au–C(12) = 2.613(6), Mo–C(1) = 2.357(6), Mo–C(2) = 2.320(6), Mo–C(3) = 2.314(6), Mo–C(4) = 2.350(7), Mo–C(5) = 2.391(6), Mo–C(10) = 1.966(6), Mo–C(11) = 1.954(6), Mo–C(12) = 1.969(7), O(1)–C(10) = 1.159(7), O(2)–C(11) = 1.158(7), O(3)–C(12) = 1.163(7), N···Cl = 2.976(5), P–Au–Mo = 174.47(4), C(10)–Mo–C(12) = 105.8(2), C(10)–Mo–C(11) = 80.4(2), C(11)–Mo–C(12) = 82.7(2), C(11)–Mo–Au = 120.70(17), C(10)–Mo–Au = 63.57(17), C(12)–Mo–Au = 65.76(16), O(1)–C(10)–Mo = 171.6(5), O(2)–C(11)–Mo = 179.5(6), O(3)–C(12)–Mo = 172.9(5).

$(\text{CO})_3(\eta^5\text{-Cp})$ (**21**).²⁰ Complexes **5**, **6**, and **8** were characterized by single-crystal X-ray crystallography; the four-legged piano-stool structures of these substances are shown in Figures 6–8, respectively. The structure of **6** differs from that of **5** by doubling the contents of the unit cell to one with $Z = 8/Z' = 2$ in $P2_1/c$ (**5** was found in $P2_1/n$); the two unique cation/anion pairs of **6** were found with a pseudoinversion relationship.³³ The Au–M distances of **5** (2.7063(5) Å), **6** (2.7060(5), 2.7121(5) Å), **8** (2.7208(6) Å), **19** (2.710(1) Å),³⁴ **20** (2.7121(5) Å),³² and **21** (2.698(3) Å)³⁵ are nearly uniform. Important average distances (Å) such as M–C(dienyl) (**5**, 2.35(3); **6**, 2.34(3); **8**, 2.33(3) Å), M–C(O) (**5**, 1.963(8); **6**, 1.958(7); **8**, 1.947(1) Å), and C–O (**5**, 1.160(3); **6**, 1.17(1); **8**, 1.167(12) Å) are statistically identical, as expected. In each complex, the $\eta^5\text{-Cp}$ engages in minor tilting away from the AuPPh_3 ligand; the pendant group exerts no perceptible steric impact on metal–Cp binding. For example, in **5**, C(5) is ~ 0.077 Å ($\sim 13\sigma$) farther from Mo than C(3); the M–C(1) and M–C(4) distances are nearly uniform. The $\text{AuM}(\text{CO})_3$ geometries of **5**, **6**, and **8** are very similar; the structural parameter that exhibits the largest variation is the trans C(11)–M–Au angle. However, the largest difference in this angle among these complexes is only $\sim 6.2^\circ$, between that of **6** (cation

(33) In order for this doubling to occur, half of the inversion centers become general sites. On the basis of the W atom positions the pseudoinversion center is located at (0.2426 0.4948 0.2378). The x and y coordinates of this pseudoinversion center are sufficiently far from the $1/4$ fractional coordinates as to not hamper the least-squares refinement of **6**. Drawings that compare the unit cells of **5** and **6** are in the Supporting Information.

(34) Pethe, J.; Maichle-Mössmer, C.; Strähle, J. *Z. Anorg. Allg. Chem.* **1997**, 623, 1413.

(35) Wilford, J. B.; Powell, H. M. *J. Chem. Soc. (A)* **1969**, 8.

(31) Braunstein, P.; Cura, E.; Herberich, G. E. *J. Chem. Soc., Dalton Trans.* **2001**, 1754.

(32) Strunin, B. N.; Grandberg, K. I.; Andrianov, V. G.; Setkina, V. N.; Perevalova, E. G.; Struchkov, Y. T.; Kursanov, D. N. *Dokl. Akad. Nauk SSSR* **1985**, 281, 599.

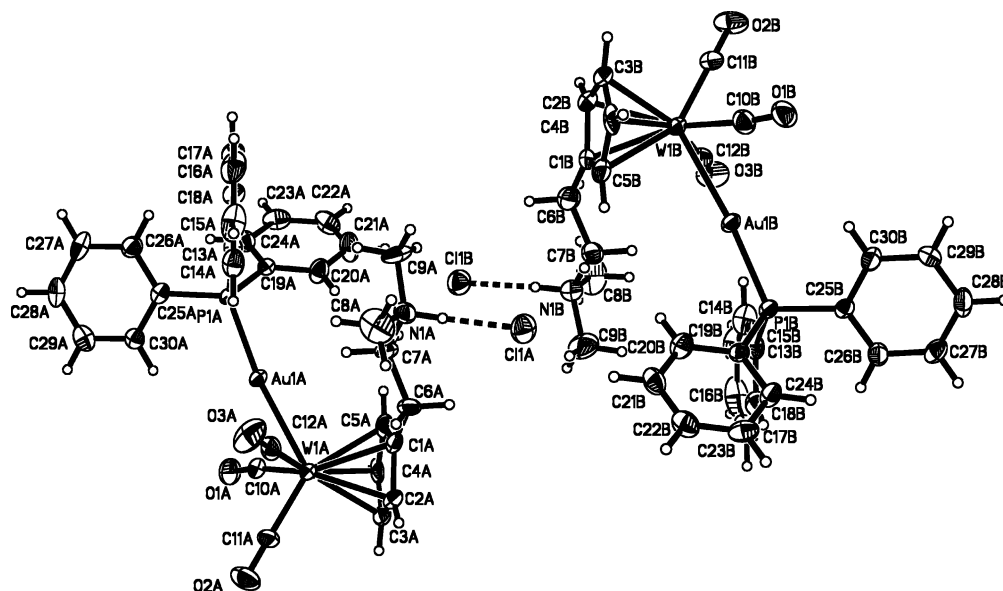


Figure 7. Molecular structure of the unique cation/anion pairs of **6** (50% thermal ellipsoids). Selected bond lengths (Å) and angles (deg): Au–W(A) = 2.7121(5), Au–W(B) = 2.7060(5), Au–C(10A) = 2.553(7), Au–C(12A) = 2.660(7), Au–C(10B) = 2.560(7), Au–C(12B) = 2.659(7), W(A)–C(dienyl) (av) = 2.35(3), W(B)–C(dienyl) (av) = 2.34(3), W(A)–C(O) (av) = 1.957(5), W(B)–C(O) (av) = 1.96(1), C(A)–O (av) = 1.16(1), C(B)–O (av) = 1.17(2), N(A)⋯Cl(A) = 2.978(6), N(B)⋯Cl(B) = 2.987(6), P–Au–W(A) = 171.89(5), P–Au–W(B) = 174.37(4), Au–W(A)–C(11A) = 121.8(2), Au–W(B)–C(11B) = 123.64(19), C(10A)–W–C(11A) = 81.2(3), C(10B)–W–C(11B) = 80.7(3), C(11A)–W–C(12A) = 81.8(3), C(11B)–W–C(12B) = 82.5(3), C(12A)–W–C(10A) = 106.6(3), C(12B)–W–C(10B) = 105.1(3), O(1A)–C(10A)–W = 171.8(6), O(1B)–C(10B)–W = 173.6(6), O(2A)–C(11A)–W = 178.5(7), O(2B)–C(11B)–W = 179.6(6), O(3A)–C(12A)–W = 175.6(6), O(3B)–C(12B)–W = 174.5(6).

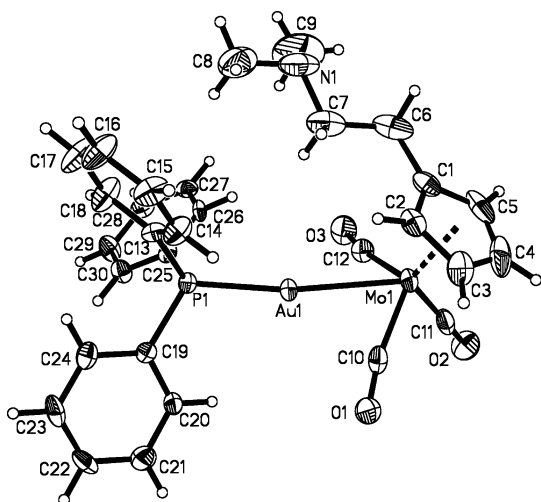


Figure 8. Molecular structure of **8** (50% thermal ellipsoids). Selected bond lengths (Å) and angles (deg): Au–Mo = 2.7208(6), Au–C(10) = 2.547(6), Au–C(12) = 2.524(6), Mo–C(1) = 2.345(6), Mo–C(2) = 2.362(6), Mo–C(3) = 2.351(6), Mo–C(4) = 2.308(7), Mo–C(5) = 2.302(6), Mo–C(10) = 1.947(6), Mo–C(11) = 1.946(7), Mo–C(12) = 1.947(7), O(1)–C(10) = 1.176(6), O(2)–C(11) = 1.171(7), O(3)–C(12) = 1.153(7), P–Au–Mo = 171.25(4), C(10)–Mo–C(12) = 107.4(3), C(10)–Mo–C(11) = 83.1(3), C(11)–Mo–C(12) = 81.5(3), C(11)–Mo–Au = 117.45(19), C(10)–Mo–Au = 63.62(17), C(12)–Mo–Au = 62.93(18), O(1)–C(10)–Mo = 169.4(5), O(2)–C(11)–Mo = 179.0(6), O(3)–C(12)–Mo = 170.3(6).

B) and **8**. The influence of crystal-packing forces on AuM(CO)₃ fragment geometry cannot be discounted, as the C(11)–W–Au angles of the unique cations of **6** are significantly different (1.84°, ~9σ). The Au to adjacent CO carbon distances range from 2.524(6) to 2.660(7) Å in **5**, **6**, and **8**. These lengths, coupled with the unifor-

mity of M–C(O) and C–O distances, and O–C–M angles such as those in **18**, rule out significant carbonyl–Au semibridging interactions in **5**, **6**, and **8**. The relatively acute O(1)–C(10)–Mo angle of **8** (169.4(5)°) is similar to that found for a semibridging carbonyl ligand in [Ti(AuPEt₃)(CO)₆][−] (169.45(6)°).³⁶ Crystal-packing forces are responsible for this angle in **8**, as O1 and its symmetry equivalent have a close contact of 2.85 Å.

Concluding Remarks

Reactions of acetic acid and in situ Na[M(CO)₃(η⁵-Cp^N)] afford zwitterionic organometalates **1–3** that engage in tight ion-pairing interactions. These zwitterions exhibit spectroscopic and structural features consistent with N–H⋯M hydrogen bonding in solution and the solid state. In this regard, complexes **1–3** join **13** as the only substances containing hydrogen bonds with zerovalent group VI metal acceptors prepared to date. The interaction between the separated charges in **1–3** lowers the electronic ground state of these zwitterions, rendering the formally negatively charged metal centers less Brønsted basic and nucleophilic relative to [M(CO)₃(η⁵-Cp)][−]. This attenuation was examined by investigating reactions of **1–3** with strong acids and triphenylphosphinegold(I) chloride. The only isolable salt from reactions of these zwitterions and hydrochloric acid was **4**, consistent with metal carbonyl anion Brønsted basicity increasing down a column. Complexes **5** and **6** were accessible by reactions of **2** and **3** with Ph₃PAuCl and **8** and **9** with hydrochloric acid. The analogous Cr salt could not be obtained despite the existence

(36) Fischer, P. J.; Young, V. G., Jr.; Ellis, J. E. *Chem. Commun.* 1997, 1249.

of neutral **7**. This study emphasizes the importance of salt elimination as a contribution to the driving force for formation of $MH(CO)_3(\eta^5-Cp)$ and $M(AuPPh_3)(CO)_3(\eta^5-Cp)$ complexes. Reactions of $Na[M(CO)_3(\eta^5-Cp)]$ and RX are commonly employed to synthesize complexes containing $M-R$ bonds with concurrent formation of insoluble NaX . Precipitation of alkali metal salts does not accompany these reactions of **1–3**. This study provides more examples of metal centers with modulated reactivity due to an intramolecular charge separation. Further studies of metal carbonyl anions containing Cp^N and related ligands are underway in this laboratory.

Acknowledgment. The donors of the Petroleum Research Fund, administered by the American Chemi-

cal Society (ACS PRF 39928-GB3), and an award from Research Corp. (CC5932) supported this research. We are grateful to these agencies and Macalester College. We are indebted to Benjamin E. Kucera and William W. Brennessel (Crystallographic Laboratory). P.J.F. thanks Professors Robert Angelici and Gerard Parkin for helpful discussions.

Supporting Information Available: Text giving additional experimental details, unit cell drawings of **5** and **6**, and crystallographic data for **1–8** compiled in tables; these data are also given as CIF files. This material is available free of charge via the Internet at <http://pubs.acs.org>.

OM050484D